Trajectory Duplication Using Relative Position Information For Automated Ground Vehicle Convoys

William Travis
Samuel Ginn College of Engineering
GPS and Vehicle Dynamics Lab
Auburn University
Auburn, Alabama 36849
Email: traviwe@auburn.edu

David M. Bevly
Samuel Ginn College of Engineering
GPS and Vehicle Dynamics Lab
Auburn University
Auburn, Alabama 36849
Email: bevlydm@auburn.edu

***Abstract*—A strategy to enhance the accuracy of path following for autonomous ground vehicles in a convoy is presented. GPS carrier measurements are used to estimate relative position with sub-two centimeter accuracy and a change in position to millimeter accuracy. These estimates are used in conjunction with three methods presented that enable a following vehicle to replicate a lead vehicle's path of travel while both are in motion and not in sight of one another. Accuracies of the methods achieved in simulation are shown with discussion on the benefits and shortcomings of each method. Simulation results show a 1.6 meter error at a 50 m following distance. Discussion explains the inaccuracies are due to the limitations inherent in the selected vehicle controller and not necessarily in the trajectory duplication methods.**

I. Introduction

The ability to precisely follow another vehicle with large separation distances would have an immediate impact on ground vehicle systems operated by the military and future automated civilian vehicle systems. A convoy of unmanned ground vehicles (UGVs) could be controlled by a single driver and operational efficiency could be improved by freeing more personnel to handle other tasks. In high risk scenarios, such as traveling through a field with unexploded ordinance (UXO), safety could be improved by having a fleet of vehicles replicate the path driven by a mine clearing vehicle or a vehicle with an on-board UXO detection system.

Many current solutions to vehicle following require vehicles to be in sight of one another so perception sensors, such as laser scanners or cameras, can obtain range and bearing information from the following to the lead vehicle [1]–[3]. However, the Global Positioning System (GPS) can be used to obtain this same information with exceptional accuracy [4], [5]. Previous works in the areas of formation flight [6], [7]; automated aircraft refueling (AAR) [8]; the Joint Precision Approach and Landing System (JPALS) [9], [10]; and ship flexure measurement [11] have derived similar methods to produce relative position information with accuracies on the order of two centimeters.

This work attempts to answer the following question: can the accurate relative position information from GPS be used to provide a means to precisely follow a path driven by an out of sight lead vehicle? Presented in this paper are three methods that can be used to replicate a lead vehicle's trajectory. Two require relatively short following distances, and the third presents a modification to the first two methods to significantly extend following distances. An explanation of the algorithms necessary to implement the three methods and their performance metrics are given. Simulation results are provided with discussion to explain the achieved performance of the path duplication methods. This work is outlined as follows:

- Section II discusses the vehicle controller derivation.
- Section III gives an overview of the relative positioning algorithm and its performance.
- Section IV describes the three methods that enable a following vehicle to drive the same path as a lead vehicle while both are in motion.
- Section V presents another algorithm that accurately estimates the change in position, which is required by the third method presented in Section IV. Achieved accuracies are listed.
- Section VI shows the results of the simulation, and a discussion is offered to provide insight into the observed accuracies.

II. Vehicle Controller

A simplistic waypoint based heading controller was used to initially determine the feasibility of the trajectory duplication methods discussed later in Section IV. To follow a path, a desired vehicle heading or yaw angle is calculated using the vehicle's current position and a selected reference point ahead of the vehicle. The vehicle drives towards the selected reference point as the yaw error approaches zero. New reference points are chosen as they come within a predetermined distance from the vehicle forcing the vehicle to drive around a path, rather than in a straight line. Human drivers alter their "look ahead distance" based on the speed they are traveling. In a parking lot environment, focus is placed in an area close to the vehicle. However in a highway environment, the area of focus could be a hundred meters from the vehicle. This concept is intuitive, but the outcome is an increase in effective damping of the system response as the distance increases. Therefore, the predetermined distance can be a function of vehicle speed to not only mimic human driving, but to soften the response to variations in the reference point.

A classical proportional-derivative (PD) controller can be used to drive the yaw error to zero. For this work, the bicycle model was used to simulate the following vehicle and derive the control gains. This model incorporates lateral vehicle motion, and therefore provides more realistic dynamics (assuming the vehicle operates within the linear region of its tire) [12]. The following transfer function describes the steer angle to yaw angle dynamics:

$$\frac{\psi(s)}{\delta(s)} = \frac{n_1 s + n_0}{s^3 + d_2 s^2 + d_1 s} \tag{1}$$

where the coefficients consist of vehicle parameters and speed.

$$n_1 = \frac{aC_{\alpha f}}{J_z} \qquad n_0 = \frac{aC_{\alpha f}C_0 - C_1 C_{\alpha f}}{mV}$$

$$d_2 = \frac{C_0 J_z + mC_2}{J_z mV} \qquad d_1 = \frac{C_0 C_2 - C_1^2 - C_1 mV^2}{J_z mV^2}$$

Parameter values were determined for a 2003 Infiniti G35 in a previous, but unrelated work [13].

Only two of the three closed loop poles are controllable with a PD controller. The third pole approaches the imaginary axis of the S-plane as speed increases. Fortunately, this pole remains stable at reasonable speeds, legitimizing the sufficiency of the PD controller. If a desired yaw rate is known, it can be fed forward with knowledge of the vehicle's understeer gradient (K_{us}) and wheelbase (L) to eliminate steady state errors while turning. The controlled input is shown below with the PD and feed-forward terms.

$$\delta = k_p\left(\psi_R - \psi\right) + k_d\left(\dot{\psi_R} - \dot{\psi}\right) + \left(\frac{L}{V} + K_{us}V\right)\dot{\psi_R} \tag{2}$$

This type of controller was modified to follow a vehicle, rather than a pre-existing path defined by waypoints. Implementation of the controller follows the above explanation of a generic path following controller, but the manner in which the reference points are generated is different. For this work, reference points, and therefore the desired vehicle yaw angle, were constructed as functions of the relative angles between the following and lead vehicles. Control gains were derived to keep two closed loop poles at a natural frequency of 1 Hz with a damping ratio of 0.707.

III. Relative Position Estimation with DRTK

By determining the relative position between the lead and following vehicles, the relative angles can easily be obtained to generate desired yaw angles for the following vehicles. A *Real-Time Kinematic* (RTK) system is a form of *differential GPS* (DGPS) that differences out common mode errors between GPS receivers in close proximity ($<$20 km) to obtain a high accuracy position solution. Typically, a static receiver is placed at a known location, often referred to as a base station. A *relative position vector* (RPV), or *baseline* vector, is determined with high accuracy between the base station and a possibly dynamic roving receiver by processing GPS range measurements. The RPV is then added to the known position of the base station to produce a highly accurate global position solution.

To increase the number of scenarios in which following vehicles replicate a lead vehicle's path of travel, it is desirable to remove the constraint of having a fixed base station. A *Dynamic base RTK* (DRTK) system removes the requirement of operating a static receiver when calculating an accurate RPV at the cost of losing the accurate global position information.

A. DRTK Algorithm

The DRTK algorithm operates in principle like a typical RTK algorithm; errors correlated in time and across space are differenced out using multiple receivers to determine the position between those receivers. To understand the subsequent derivation and appreciate the accuracies achieved by RTK and DRTK, mathematical models of the code and carrier based range measurements at time t_k, as defined by [14], are given:

$$\begin{aligned}\rho_A^j(t_k) =& \|\vec{r}_A^j(t_k)\| + \lambda\gamma(t_k) + \lambda\xi(t_k) + c\delta t_A(t_k) \\ &- c\delta t^j(t_k) + \epsilon_\rho(t_k)\end{aligned} \tag{3}$$

$$\begin{aligned}\phi_A^j(t_k) =& \lambda^{-1}\|\vec{r}_A^j(t_k)\| - \gamma(t_k) + \xi(t_k) + a_A^j(t_k) \\ &+ f\delta t_A(t_k) - f\delta t^j(t_k) + \epsilon_\phi(t_k)\end{aligned} \tag{4}$$

The variables are defined as follows:

ρ_A^j	the measured range (pseudorange), in meters, from receiver A to satellite j
ϕ_A^j	the measured carrier signal phase, in cycles, from receiver A to satellite j
r_A^j	the true range from satellite j to receiver A, in meters
λ	the wavelength of the carrier, in meters
γ	the ionospheric delay/advancement, in cycles
ξ	the tropospheric delay, in cycles
δt_A	the clock error, in seconds, at the receiver
δt^j	the clock error, in seconds, at satellite j
a_A^j	the integer number of cycles from receiver A to satellite j
f	the carrier frequency
ϵ	system noise, including multipath

Most GPS receivers use the code modulated onto the carrier to determine the value of the pseudorange between the receiver antenna and satellite. However, phase measurement accuracy is significantly better than the pseudorange accuracy. Typical accuracies for pseudorange measurements are half a meter, while accuracies for the phase measurement are around five millimeters [14]. The phase measurement is also more robust to multipath error [15]. In order to use the phase measurements to obtain higher accuracy position estimates, the integer number of cycles between the user and satellite must be resolved. This value is commonly known as the integer ambiguity.

The DRTK algorithm uses a combination of the pseudorange and carrier phase measurements in a discrete, linear Kalman filter [16] to estimate the relative ambiguity between receivers. Once the ambiguities are fixed, a least squares routine is used to estimate the baseline vector between receivers.

The state vector, x, of length n used in the Kalman filter contains relative position, velocity, and floating ambiguity estimates.

$$x_{NC1} = [\dot{\vec{b}}_{1x3} \quad \vec{b}_{1x3} \quad \hat{a}_{1xm}]^T \tag{5}$$

In the above equation, b and $\dot{b}$ are relative position and velocity vectors in Earth Centered, Earth Fixed (ECEF) coordinates. The vector of length m containing floating point ambiguities is denoted by $\hat{a}$. The length of the vector is determined by the number of double differenced carrier phase measurements available. This and the integerization process of the floating point ambiguity estimates will be discussed later.

The state dynamics matrix F is given by:

$$F_{nxn} = \begin{bmatrix} \frac{1}{\tau}I_{3x3} & 0_{3x3} & 0_{3x3} \\ I_{3x3} & 0_{3x3} & 0_{3x3} \\ 0_{mx3} & 0_{mx3} & 0_{mx3} \end{bmatrix} \tag{6}$$

The matrix contains several sub matrices that relate each sub vector in the state vector to its derivative. The time constant τ is a tuning parameter based on the dynamics of each receiver, I is an identity matrix, and 0 is an appropriately sized matrix of zeros.

The continuous process noise covariance matrix, $Q(t)$ is constructed to capture the correlation between position and velocity. The tuning parameters σ_Q and σ_a can be altered to adjust the level of filtering on the estimated states.

$$Q(t)_{nxn} = \begin{bmatrix} \sigma_Q I_{3x3} & 0_{3x3} & 0_{3x3} \\ 0_{3x3} & \sigma_Q I_{3x3} & 0_{3x3} \\ 0_{mx3} & 0_{mx3} & \sigma_a I_{mx3} \end{bmatrix} \tag{7}$$

The matrices in Equations 6 and 7 can be discretized by the method presented by van Loan [17] since this is a fixed parameter system.

$$\mathcal{A}_{2nx2n} = \begin{bmatrix} -F & GQ(t)G^T \\ 0 & F^T \end{bmatrix} \Delta t \tag{8}$$

For this system, $G = I_{nxn}$. The discretized state transition matrix and process noise covariance matrix can be extracted using the following relationship:

$$e^{\mathcal{A}} = \begin{bmatrix} \mathcal{B} & \Phi^{-1}Q \\ 0 & \Phi^T \end{bmatrix} \tag{9}$$

Carrier phase and pseudorange measurements are used in the measurement update, but first the error terms must be addressed. A single difference is formed by subtracting measurements from two receivers observing the same satellite at the same instance in time. If the receivers are in close proximity (<20 km), an assumption can be made that the atmospheric errors observed at the two stations are the same. It is important to note that some situations, such as high ionospheric activity or severe weather, can potentially falsify this assumption [18]. Using Equation 4, a single difference for the carrier measurement can be calculated.

$$\begin{aligned} \Delta\phi^j_{AB}(t_k) =& \phi^j_B(t_k) - \phi^j_A(t_k) \\ =& \lambda^{-1}r(t_k) + a^j_{AB} + f\delta t_B(t_k) \\ & - f\delta t_A(t_k) + \epsilon_{\Delta\phi}(t_k) \end{aligned} \tag{10}$$

Notice the atmospheric and satellite clock errors have been removed, but the noise has been increased. A vector of single differences of observations from different satellites can be represented as follows:

$$\Delta\phi(t_k)_{mx1} = [\phi^j_{AB}(t_k) \quad \dots \quad \phi^n_{AB}(t_k)]^T \tag{11}$$

Assuming the phase measurements are linearly independent, the covariance of the single differenced phases can be derived [15].

$$\begin{aligned} R_{\Delta\phi_{mxm}} =& E[(\Delta\phi(t_k) - \overline{\Delta\phi}(t_k))^2] \\ =& 2\sigma^2_{\epsilon_\phi} I_{mxm} \end{aligned} \tag{12}$$

This same procedure should be applied to the Equation 3 to produce a vector of single differenced pseudorange measurements, $\Delta\rho(t_k)_{mx1}$, and its associated covariance, $R_{\Delta\rho_{mxm}}$. The remaining error sources are the receiver clock biases and noise in the single differenced equations. An integer ambiguity is present in the carrier phase equations.

A double difference is formed by differencing two single differences, thus removing the error due to receiver clock bias:

$$\begin{aligned} \nabla\Delta\phi^{jz}_{AB}(t_k) =& \Delta\phi^z_{AB}(t_k) - \Delta\phi^j_{AB}(t_k) \\ =& \lambda^{-1}r(t_k) + a^{jz}_{AB} + \epsilon_{\nabla\Delta\phi}(t_k) \end{aligned} \tag{13}$$

A vector of double differences is formed by selecting a "base" single difference (denoted by satellite z) and differencing all the other single differences with it. The intuitive selection would be the single difference of the satellite closest to the zenith, as its signal travels the shortest distance through the atmosphere and theoretically subjected to less interference.

$$\nabla\Delta\phi(t_k)_{mx1} = [\Delta\phi^z_{AB}(t_k) - \Delta\phi(t_k)]^T \tag{14}$$

The covariance matrix for the double differenced phases can be derived like the covariance of the single differenced covariances in (12). Again, the noise is increased and the measurements become correlated.

$$\begin{aligned} R_{\nabla\Delta\phi_{mxm}} &= E[(\nabla\Delta\phi(t_k) - \overline{\nabla\Delta\phi}(t_k))^2] \\ R_{\nabla\Delta\phi_{ij}} &= \begin{cases} 4\sigma^2_{\epsilon_\phi} & \text{for } i = j \\ -2\sigma^2_{\epsilon_\phi} & \text{for } i \neq j \end{cases} \end{aligned} \tag{15}$$

Again, the vector of pseudorange double differences and resulting covariance matrix, denoted by $\nabla\Delta\rho(t_k)_{mx1}$ and $R_{\nabla\Delta\rho_{mxm}}$, respectively, can be formed using the same procedure.

Once the double differenced carrier phase and pseudorange measurements are formed, the measurement vector and measurement covariance matrix for the Kalman filter can be constructed. The measurement vector z is formed using the vector of double differenced carrier phase and pseudorange measurements, where both are in units of cycles.

$$z_{2mx1} = \left[\lambda^{-1}\nabla\Delta\rho(t_k) \quad \nabla\Delta\phi(t_k)\right]^T \tag{16}$$

The covariance matrix $\mathbf{R}$ is constructed using the individual double differenced covariance matrices.

$$R_{2mx2m} = \begin{bmatrix} R_{\nabla\Delta\rho_{mxm}} & 0_{mxm} \\ 0_{mxm} & R_{\nabla\Delta\phi_{mxm}} \end{bmatrix} \tag{17}$$

Unit vectors from the user to each satellite must be formed to form the measurement matrix. A single unit vector can be formed by dividing the range components in the ECEF X, Y, and Z direction by the magnitude of the range.

$$u^j_{1x3} = \frac{\vec{r}^{\,j}_{1x3}}{\|\vec{r}^{\,j}\|} \tag{18}$$

Once all the unit vectors are determined, they should be subtracted from the unit vector of the "base" satellite. Division by the carrier wavelength, λ, converts the units from meters to cycles.

$$\Delta U_{mx3} = \lambda^{-1} \begin{bmatrix} u^z - u^j \\ \vdots \\ u^z - u^n \end{bmatrix} \tag{19}$$

Finally, the measurement matrix H is constructed using ΔU as follows:

$$H_{2mxn} = \begin{bmatrix} 0_{mx3} & \Delta U_{mx3} & 0_{mxm} \\ 0_{mx3} & \Delta U_{mx3} & I_{mxm} \end{bmatrix} \tag{20}$$

Given enough satellites, the Kalman filter, as described, will estimate a relative velocity, relative position, and a non-integer number of carrier cycles. It is crucial to obtain integer values for the cycle ambiguity if a high precision RPV is desired. The LAMBDA method [19] has been proven to provide the highest probability of acquiring the correct set of integer ambiguities among many integer ambiguity acquisition algorithms [20]. The floating ambiguities, $\hat{a}$, and their associated covariance from the Kalman filter are input into the LAMBDA algorithm. It decorrelates the ambiguities to produce a minimized search space and outputs the possible integerized solution sets, $(\tilde{a})$, contained within that space with their covariance matrices $(P_{\tilde{a}})$ [21]. A common method to determine the correct ambiguity set is a ratio test between the square norms of the integer ambiguities, where the best set is deemed correct if the ratio is above some value, κ [6], [22]. In the equation below, a ratio of the best set to the second best set is calculated. The value for κ is selected by the user and is generally 1.5 or 2.

$$\frac{\left[\hat{a} - \tilde{a_2}\right]^T P^{-1}_{\tilde{a_2}} \left[\hat{a} - \tilde{a_2}\right]}{\left[\hat{a} - \tilde{a_1}\right]^T P^{-1}_{\tilde{a_1}} \left[\hat{a} - \tilde{a_1}\right]} \underset{reject}{\overset{accept}{\gtrless}} \kappa \tag{21}$$

Future work will replace this test with a Bootstrapping technique to increase the integrity of the ambiguity solution [23].

Once the integer ambiguities have been correctly determined, a least squares procedure is used to determine a precise RPV. The measurement vector consists of only the double differenced carrier measurements with the ambiguity removed. The measurement matrix is compensated to reflect the reduced size of the measurement vector.

$$\vec{b}_{3x1} = \left[\Delta U^T \Delta U\right]^{-1} \Delta U^T \left[\nabla\Delta\phi - \tilde{a}\right] \tag{22}$$

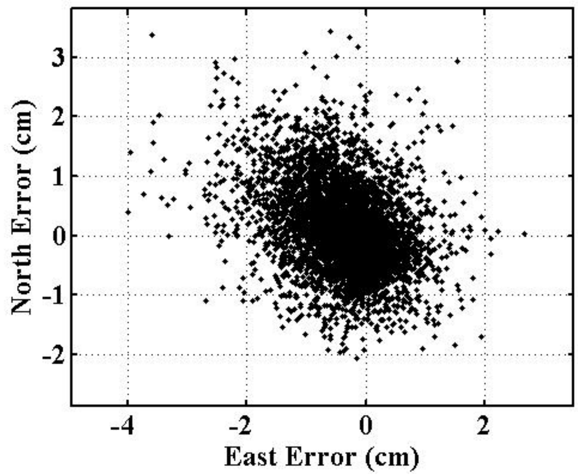

Fig. 1. Displayed is the error in the North and East components of the RPV estimated with the DRTK algorithm. The standard deviations were 0.70 cm and 0.68 cm, respectively, with an approximate 2 m baseline during the test.

B. DRTK Performance

The RPV estimated with the DRTK algorithm was compared to the position difference of the RTK position solution from two moving NovAtel Propak-V3 receivers. GPS range data and the RTK positions were logged at 5 Hz for twenty minutes while the receivers were in motion. One receiver was on a vehicle, and the other receiver was on a trailer towed by the vehicle; therefore the magnitude of the RPV remained constant, but the ECEF components of the RPV varied.

Figure 1 displays error in the North and East direction after the RPV had been rotated from the ECEF to East, North, Up (ENU) coordinate frame. The one sigma error bounds for this data set were 0.70 cm and 0.68 cm in the North and East directions. The small error can be attributed to the relatively short baseline between the receivers, which was approximately two meters for this test.

IV. Reference Angle Generation Methods

In order to duplicate a vehicle's path of travel using the controller described in Section II, reference points for the following vehicles must be generated on the fly. Perhaps the easiest method of generating reference points is to broadcast the lead vehicle's current position to the following vehicles. However, the accuracy of a standalone receiver is, at best, three meters. The following vehicles could be six or more meters from the true path as they approach the reference points. If an RTK system is available, this method would actually work well as the positional accuracy would be reduced by an order of magnitude. A six centimeter path error could be tolerable in many scenarios. The requirement of a fixed base station could

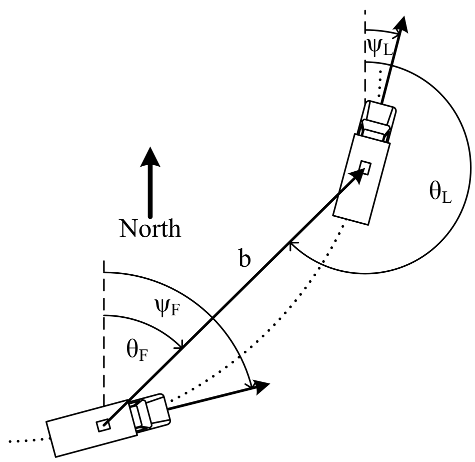

Fig. 2. The schematic for the Trailer Method is shown. By controlling the following vehicle's yaw angle to the relative angle between the vehicle's, the following vehicle acts as if it were in tow by the lead vehicle. The relative angle can be calculated once the RPV is known.

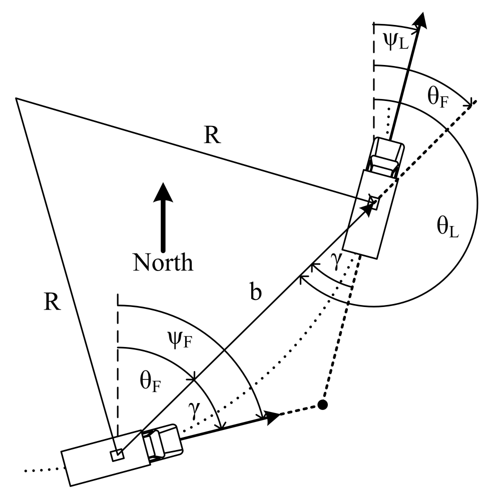

Fig. 3. The Extended Hitch Trailer Method controls the following vehicle to a point behind the lead vehicle to force the following vehicle to turn about the same radius as the lead vehicle. The reference angle for this method relies on the RPV and the yaw angle of the lead vehicle.

reduce the feasibility of autonomous trajectory duplication. Therefore, methods that do not rely simply on broadcasting and maintaining a log of lead vehicle position need to be developed to broaden the application spectrum for automated ground vehicle convoys.

The following three subsections present methods that rely on the DRTK RPV to generate reference points for the controller. The first two subsections present methods that allow for short following distances. The third subsection outlines a method to significantly extend following distances by modifying the first two methods.

A. Short Distance Following

1) Trailer Method: The simplest method to generate a reference for control with knowledge of the RPV, $\vec{b}$, between two vehicles is to control the following vehicle's yaw angle, ψ_F, to the relative angle between the vehicles, θ_F, as seen in Figure 2. The following vehicle mimics a trailer in tow by the lead vehicle, and the trailer hitch and GPS antenna on the lead vehicle are collocated. Since the components of the RPV are known and can be realized in a local ENU or NED frame, the relative angle from North between the following vehicle to the lead vehicle can be easily calculated.

$$\theta_F = \tan^{-1}\left(\frac{b_E}{b_N}\right) \tag{23}$$

Once the relative angle is known, it is given to the controller as the desired yaw angle.

$$\psi_R = \theta_F \tag{24}$$

The simplicity of this method is both beneficial and harmful to path duplication ability:

- The Trailer Method is relatively easy to implement. The only information transferred between the vehicles is the GPS range measurements from the leader to the followers. Once the RPV is known, the relative angle, which is also the reference yaw angle, can be calculated.
- For short following distances, this method works well. Natural lags in the system can overcome the tendency to cut corners.
- The turning radius of the following vehicle will be smaller than the lead vehicle's turning radius. Therefore, path following error will be zero only when the lead vehicle drives straight.
- Lateral path error grows as the following distance increases because the turning radii become more dissimilar.

2) Extended Hitch Trailer Method: Work presented by Ng in [2] showed that projecting the reference point behind the lead vehicle, creating a "virtual hitch", reduced the lateral error during a turn. This method was adapted and modified to make use of the accurate RPV. It was also shown in [2] that the optimal location for the hitch point was at a location equidistant to both lead and following vehicles. This ensured both vehicles were on a path of the same turning radius, R. This concept is seen in the schematic for this method in Figure 3.

To create the reference angle, the reference point is placed behind the lead vehicle along its longitudinal axis such that it forms an isosceles triangle with the location of the following vehicle. The reference yaw angle, ψ_R, can be derived with knowledge of the non-vertex angle in the isosceles triangle, γ, and the relative angle between the vehicles, θ_F.

Analysis of the angles about the following vehicle shows that the following vehicle's yaw angle should be controlled to the angle to the reference point. Therefore, the reference angle can be denoted by the following equation:

$$\psi_R = \theta_F + \gamma \tag{25}$$

If the relative angle of the following vehicle is projected to the lead vehicle, the non-vertex angle can be calculated using the lead vehicle's yaw angle.

$$\gamma = \theta_F - \psi_L \tag{26}$$

Combining Equations 25 and 26 yields the following equation for the reference angle:

$$\psi_R = 2\theta_F + \psi_L \tag{27}$$

Therefore, the only necessary information needed to calculate the reference angle is the relative angle, which can be determined with the RPV as in Equation 23, and the yaw angle of the lead vehicle. The complexity has been increased over the Trailer Method because more information is necessary. However, the level of increase is only slight. The yaw angle could either be broadcast to the following vehicles with the GPS range information, or the following vehicles could use the range information to determine the lead vehicle's heading. The former solution would require a very slight increase in required communication bandwidth, while the latter would raise the computational requirements on the following vehicles.

As with the Trailer Method, trade offs exist due to the simplicity of the Extended Hitch Trailer Method.

- Projecting the reference point behind the lead vehicle creates a desired yaw angle that orients the following vehicle along a path with the same turning radius as the lead vehicle. This reduces error due to unequal turning radii, which can occur using the Trailer Method.
- The Extended Hitch Trailer Method is only slightly more complicated than the Trailer Method. The leader's yaw angle can easily be obtained.
- The following distance can be extended since the tendency to cut corners has been addressed.
- Error still exists while turning; transitions of path curvature cause the following vehicle to deviate from the intended path as it prematurely attempts to equalize the turning radii.
- Although following distances can be increased, this method breaks down when long following distances are desired.

3) Performance of the Trailer Methods: A simulation of a following vehicle tracking the path of a lead vehicle making a 100 m radius, left turn at 15 m/s with a 50 m following distance is used to illustrate the performance of the two methods previously discussed. Figure 4 shows the actual paths traveled of the lead vehicle and the following vehicle using both methods. Figure 5 displays the lateral path error of both methods. The Extended Hitch Trailer Method significantly outperforms the Trailer Method in the simulated scenario. Lateral errors exhibited are approximately two meters and ten meters, respectively. The Trailer Method caused the following vehicle to turn about a smaller radius through the entire duration of the turn, which generated large path error. The Extended Hitch Trailer Method caused the following vehicle to experience the most error as the lead vehicle transitioned from driving straight to turning, and vise versa. Any change in the yaw rate of the lead vehicle changes its turning radius. This change immediately alters the turning radius of the following vehicle, even though it should maintain a previous turning radius of the lead vehicle to maximize accuracy. The overall effect is the following vehicle turns off the path when the leader transitions from a straight to curved trajectory, and the following vehicle cuts off the remaining path when the lead vehicle transitions from a curved to straight trajectory. The magnitude of this effect is proportional to following distance; short distances reduce errors while large distances magnify them.

Realistic applications of these methods would demand short following distances. Any complexity in the path driven by

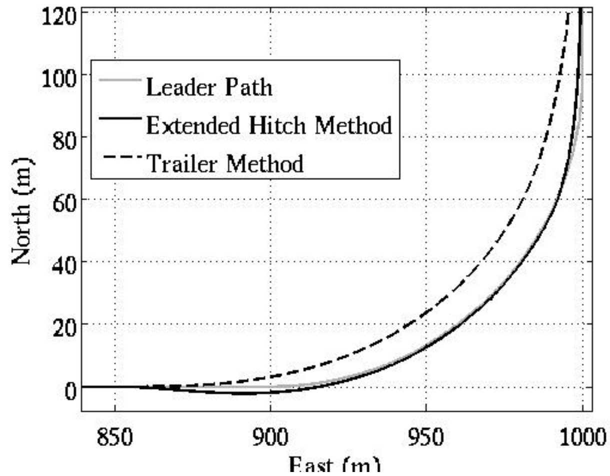

Fig. 4. The lead vehicle path (gray) is replicated using the Trailer Method (dashed) and Extended Hitch Trailer Method (solid) while the lead vehicle traveled around a 100 m radius left turn at 50 m/s. The following vehicle was simulated with a 50 m following distance. The Extended Hitch Method significantly outperforms the Trailer Method, but it still fails to replicate the exact path of the leader because of errors induced by changes in curvature.

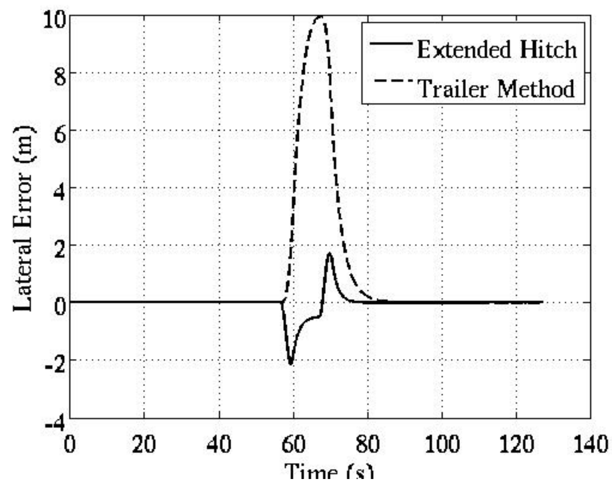

Fig. 5. Lateral error of the Trailer Method (dashed) and Extended Hitch Trailer Method (solid) when 50 m behind a lead vehicle traveling around a left 100 m radius turn at 15 m/s. Maximum path deviation is approximately 10 m and 2 m, respectively.

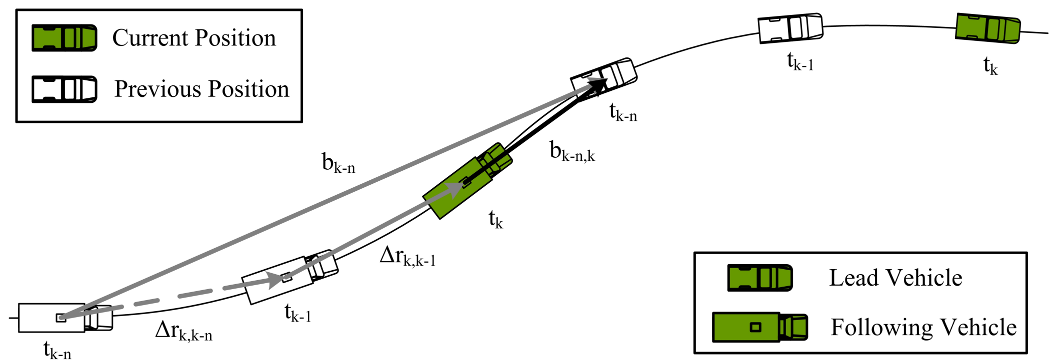

Fig. 6. By accumulating the position change at each time step of the following vehicle, the RPV between the lead and following vehicle at a previous time step can be translated to an RPV between the following vehicle at the current time step and the lead vehicle at a previous time step (black vector). This reduces the effective following distance and increases the effectiveness of previously discussed trajectory duplication methods.

the lead vehicle would effectively be filtered if the following vehicles were too far behind. Therefore, following distance would be dependent upon anticipated path complexity.

B. Long Distance Following

The amount of error experienced using the previous methods is related to the separation distance between the lead and following vehicles. Larger following distances cause the following vehicle to deviate from simplistic paths and render both methods useless for intricate paths driven by the leader. However, short following distances can allow the following vehicle to accurately repeat the leader's path. Therefore, the separation distance perceived by the following vehicle must be reduced to improve accuracy.

If the change in position of the following vehicle can be accumulated, it can be subtracted from a previous RPV. This effort reduces the perceived baseline from the follower to the leader, and the RPV is now the distance between the following vehicle at the current time and the lead vehicle at a previous time. Sufficient knowledge of past changes in position can shrink the RPV to minimize trajectory duplication error using either the Trailer Method or Extended Hitch Method. This concept is mathematically expressed as follows:

$$\vec{b}_{k,k-n} = \vec{b}_{k-n} - \sum_{j=k-n}^{k} \Delta\vec{r}_j \tag{28}$$

The change in position, $\Delta\vec{r}$, is summed from index $k-n$ to the current index k. This value is then subtracted from the RPV at index $k-n$ to determine the RPV between the follower at k and leader at $k-n$. Once the new RPV is obtained, it can be utilized as described in either of the previously mentioned methods.

This notion is graphically explained in Figure 6, where the gray lines represent measurements of the RPV and change in position at previous times and the black line represents the shortened RPV between the leader at a previous time and follower at the current time. The solid color vehicles indicate their location at the current time step, and the transparent vehicles are past locations.

Implementation of the Modified Extended Hitch Trailer Method provides the user the capability to have an automated vehicle follow and track a lead vehicle's traveled path. However, some aspects might deem the method infeasible for some applications. Pros and cons of this method are itemized below.

- The Modified Extended Hitch Trailer Method reduces the perceived relative position regardless of following distance by translating the RPV at between the follower and leader at a previous instance in time to a shortened RPV across time.
- Since the RPV has been reduced, the magnitude of the errors displayed by the Trailer Method and Extended Hitch Trailer Method is decreased.
- Longer following distances are possible regardless of path complexity since the perceived distance is reduced.
- The method is more complicated as a database of information is required. This includes RPV's, changes in position, and yaw angles of the lead vehicle.
- An additional measurement is required to determine the position change of the following vehicle.
- Any error in the change of position measurement will accumulate, potentially degrading the effectiveness of this method. Accuracy requirements of this measurement might be too stringent for some applications. The effect of errors are considered in Section VI-A.

V. Estimation of the Change in Position

The GPS carrier signal is used to achieve the necessary accuracies required to improve the usefulness of the method presented in Section IV-B. The advantage to carrier processing has already been demonstrated with the accuracy of the DRTK algorithm in Figure 1. The following algorithm description relies on similar concepts to those discussed in Section III.

A. TDCP Algorithm

The discussion on the error mitigation achieved by differencing carrier measurements across receivers and across satellites can now be amended to present another technique to reduce errors inherent in the GPS signal. *Time differenced*

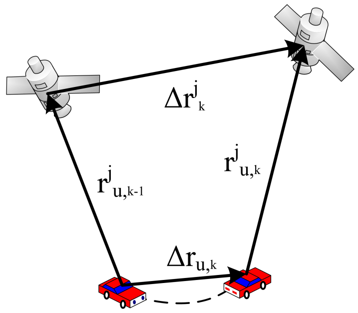

Fig. 7. The change in receiver and satellite position is captured in the difference in range measurements from the user to the satellite, assuming the time difference between measurements is small.

carrier phase (TDCP) measurements can provide a measure of change in position. Similar to differencing across receivers or satellites, differencing across time can reduce the atmospheric and satellite clock errors to negligible values and remove the integer ambiguity. The underlying stipulation is the time difference is small enough to assume all the errors are correlated.

The carrier phase measurement model from satellite j at the current and a previous time step is shown in the following equation, where τ represents the small time difference between measurements.

$$\begin{aligned}\phi_A^j(t_k) =&\lambda^{-1}(\|\vec{r}_A^j(t_k)\| - \lambda\gamma(t_k) + \lambda\xi(t_k)) + a_A^j(t_k) \\ &+ f\delta t_A(t_k) - f\delta t^j(t_k) + \epsilon_\phi(t_k)\end{aligned} \tag{29}$$

$$\begin{aligned}\phi_A^j(t_{k-\tau}) =&\lambda^{-1}(\|\vec{r}_A^j(t_{k-\tau})\| - \gamma(t_{k-\tau}) + \xi(t_{k-\tau})) \\ &+ a_A^j(t_{k-\tau}) + f\delta t_A(t_{k-\tau}) \\ &- f\delta t^j(t_{k-\tau}) + \epsilon_\phi(t_{k-\tau})\end{aligned} \tag{30}$$

The TDCP measurement is realized by subtracting Equation 30 from Equation 29. The variable t will be dropped for simplicity.

$$\begin{aligned}\phi_{A_k}^j - \phi_{A_{k-\tau}}^j =&\lambda^{-1}\left(\|\vec{r}_A^j\|_k - \|\vec{r}_A^j\|_{k-\tau}\right) \\ &+ f\left(\delta_{A_k} - \delta_{A_{k-\tau}}\right) + \epsilon_{\phi_{k,k-\tau}}\end{aligned} \tag{31}$$

The above equation can be written more succinctly as follows:

$$\Delta\phi_{A_{k,k-\tau}}^j = \lambda^{-1}\Delta\|\vec{r}_A^j\|_{k,k-\tau} + f\Delta\delta_{A_{k,k-\tau}} + \epsilon_{\phi_{k,k-\tau}} \tag{32}$$

The TDCP measurement, assuming the time difference is sufficiently small, is unaffected by atmospheric effects, satellite clock bias, and the integer ambiguity. The remaining terms are the change in the range measurements, $\Delta\|\vec{r}_A^j\|_{k,k-\tau}$, and the change in receiver clock bias, $\Delta\delta_{A_{k,k-\tau}}$. Contained in the change in range is both the change in satellite and receiver positions, as depicted by Figure 7.

Normally the use of the TDCP measurement would require a restructuring of the estimator to handle measurements at different instances in time [24], [25]. However, a method is presented in [26] that expands Equations 31 and 32 about a nominal position, $\vec{r}_{A_{0_k}}$, and clock bias, $\delta_{A_{0_k}}$, using a Taylor series. The ECEF receiver position and clock bias can be expressed as shown below.

$$\vec{r}_{A_k} = \vec{r}_{A_{0_k}} + \Delta\vec{r}_{A_k} \tag{33}$$

$$\delta_{A_k} = \delta_{A_{0_k}} + \Delta\delta_{A_k} \tag{34}$$

Incorporating Equations 33 and 34 into Equation 31 produces a TDCP equation where all but four terms are known; the remaining unknowns are the change in receiver position, $\Delta\vec{r}_{A_k}$, and change in receiver clock bias, $\Delta\delta_{A_k}$.

$$\begin{aligned}\lambda\Delta\phi_{A_{k,k-\tau}}^j =&\|\vec{r}_{A_0}^j\|_k - \|\vec{r}_A^j\|_{k-\tau}\frac{\vec{r}_{A_{0_k}}^j}{\|\vec{r}_{A_0}^j\|_k}\cdot\Delta\vec{r}_{A_k} \\ &+ c\delta_{A_{0_k}} + c\Delta\delta_{A_k} + \epsilon_{\phi_{k,k-\tau}}\end{aligned} \tag{35}$$

A weighted least squares algorithm can be used to estimate the change in position. The state vector is as follows:

$$x_{4x1} = [\Delta\vec{r}_{A_{1x3}} \quad c\Delta\delta_{1x1}]^T \tag{36}$$

The measurement vector contains the TDCP measurements and expansion terms. The variable j is used in the following equations to denote values between the receiver and satellite.

$$z_{mx1} = \lambda\Delta\phi_{A_{k,k-\tau}}^j - \|\vec{r}_{A_0}^j\|_k + \|\vec{r}_A^j\|_{k-\tau} - c\delta_{A_{0_k}} \tag{37}$$

The measurement matrix consists of the unit vectors created with the ranges from the nominal position to the satellites.

$$H_{mx4} = \begin{bmatrix} \frac{\vec{r}_{A_{0_k}}^j}{\|\vec{r}_{A_0}^j\|_k} & 1 \end{bmatrix} \tag{38}$$

The diagonal weighting matrix was constructed using a thermal noise model described in [27]. This incorporated the carrier to noise ratio, C/N_0, so the degraded signals were de-weighted.

$$W_{ii} = \left(\frac{B_n}{C/N_0}\left(1 + \frac{1}{2T_sC/N_0}\right)\right)^{-1} \tag{39}$$

A third order loop filter was assumed with a bandwidth, B_n, of 18 Hz and a predetection integration time, T_s, of five milliseconds. The reasoning for the selection of these values is thoroughly explained in [27].

B. TDCP Performance

GPS range data was collected at 5 Hz on a static NovAtel Propak-V3 receiver for 85 minutes. Dynamic data was also collected and analyzed to verify the algorithm, but static data was used to obtain more accurate error statistics. Figure 8 shows a scatter plot of the error in change in position after the estimates had been rotated to the ENU coordinate frame. The one sigma bounds in the North and East directions were 0.75 mm and 1.09 mm, respectively.

A trade off exists between measurement rate and accuracy. Measurement errors are more correlated with higher sampling rates, therefore more of the errors will be removed by the time difference. Slower sampling rates will yield less accurate results because of the lower error correlation. The full extent of accuracy versus sampling rate has not been investigated at this time.

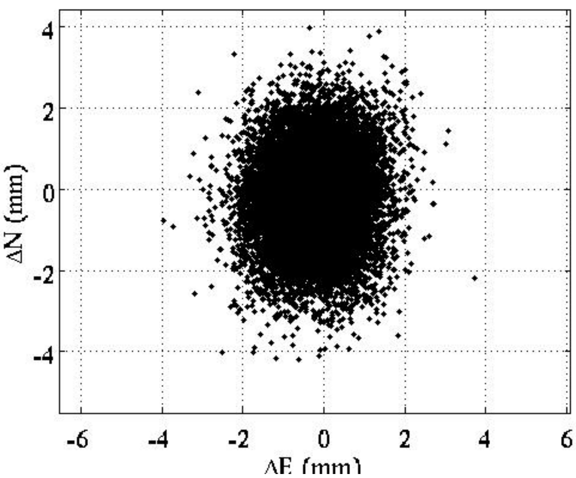

Fig. 8. TDCP performance using 85 minutes of static data logged at 5 Hz. The North standard deviation was 0.75 mm, while the East standard deviation was 1.09 mm.

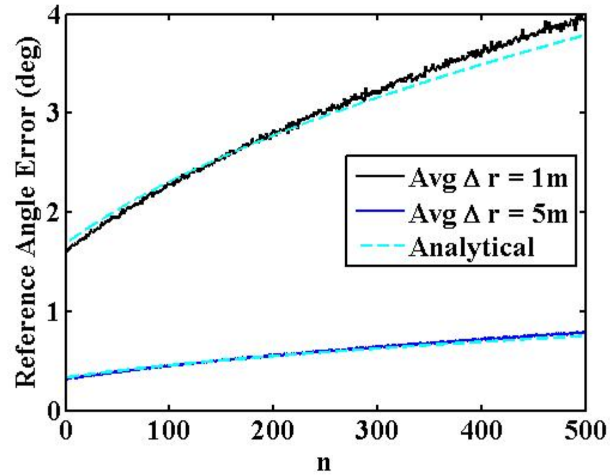

Fig. 9. Reference angle error grows as a function of the number of accumulated positions, n, and the average change in position. An analytical approximation (dashed) given in Equation 42 captures the growth while $n \leq 500$. Maximum error for an average change in position of 1 m and 5 m is 4 degrees and 0.9 degrees, respectively.

VI. Results Using the Modified Extended Hitch Trailer Method

A. Reference Error

Transferring the DRTK baseline estimate using the TDCP output increases the noise on the perceived RPV. This noise increase is proportional to the number of accumulated position changes. The following derivation analytically predicts the standard deviation of the translated RPV with the assumption the DRTK and TDCP outputs are both zero mean and uncorrelated.

$$\sigma^2_{\vec{b}_{k,k-n}} = E\left[\left(\vec{b}_{k-n} - \sum_{j=k-n}^{k} \Delta\vec{r}_j\right)^2\right]$$

$$= E\left[\vec{b}^2_{k-n}\right] - 2E\left[\vec{b}_{k-n}\sum_{j=k-n}^{k}\Delta\vec{r}_j\right] + E\left[\sum_{j=k-n}^{k}\Delta\vec{r}^2_j\right]$$

$$= E\left[\vec{b}^2_{k-n}\right] + nE\left[\Delta\vec{r}^2\right] \tag{40}$$

Solving for the standard deviation shows the standard deviation of the translated RPV is a function of the covariance of the previous RPV, $\sigma^2_{\vec{b}_{k-n}}$; the covariance of the TDCP output, $\sigma^2_{\Delta\vec{r}}$; and the number of accumulated position changes, n.

$$\sigma_{\vec{b}_{k,k-n}} = \sqrt{\sigma^2_{\vec{b}_{k-n}} + n\sigma^2_{\Delta\vec{r}}} \tag{41}$$

The translated RPV is used to generate a relative angle using Equation 23, which is then used in either Equations 24 or 27 to calculate a desired yaw angle for a following vehicle. A Monte Carlo analysis reveals the accuracy of this reference angle as a function of the number of accumulated position changes and average change in position. The results for average position changes of one meter and five meters with a 5 Hz measurement rate are shown in Figure 9. After 500 summations of the change in position measurements, the error in the reference angle is approximately four degrees when the average position change was one meter and approximately 0.9 degrees when the average position change was five meters. For reference, an average change in position of five meters at a measurement rate of 5 Hz is an average velocity of 25 m/s, and the accumulation of 500 measurements indicates a following distance of 2.5 km.

An analytical approximation of these curves is expressed by the following equation:

$$\sigma_{\psi_R} = \|\overline{\Delta\vec{r}}\|^{-1}\left(\sigma^2_{\vec{b}_{k-n}} + n\sigma^2_{\Delta\vec{r}}\right)^{\frac{9}{20}} \tag{42}$$

This approximation considers the covariance of the RPV, change in position, number of accumulated positions, and the inverse of the magnitude of the average change in position, $\|\overline{\Delta\vec{r}}\|$. Note the approximation begins to break down as the number of position accumulations increases.

B. Trajectory Duplication Performance

Position data was collected in a parking lot to generate a complex lead vehicle path. Speeds ranged from 1-15 m/s. The data was replayed in simulation, and a following vehicle attempted to track the traveled path with a 50 m separation distance while both vehicles were in motion. The Modified Extended Hitch Trailer Method was used to reduce the effective RPV between the vehicles. Measurements of the RPV and change in position were simulated at 5 Hz and corrupted with 2 cm Gaussian noise. Although this value is higher than reported statistics, it was chosen to stress the trajectory duplication method. Figure 10 shows the path traveled by both vehicles; the lead vehicle traveled the gray path and the following vehicle traveled the black path.

Figure 11 shows the lateral error between the follower vehicle and the lead vehicle's travel path. The large initial error is due to the 50 m offset between the follower position

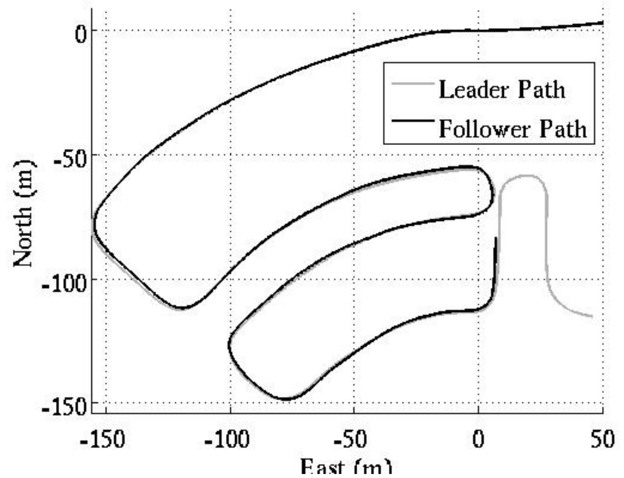

Fig. 10. Shown are the simulated trajectories of the lead (gray) and following (black) vehicles as the follower attempted to replicate the leader's path of travel with a 50 m separation distance.

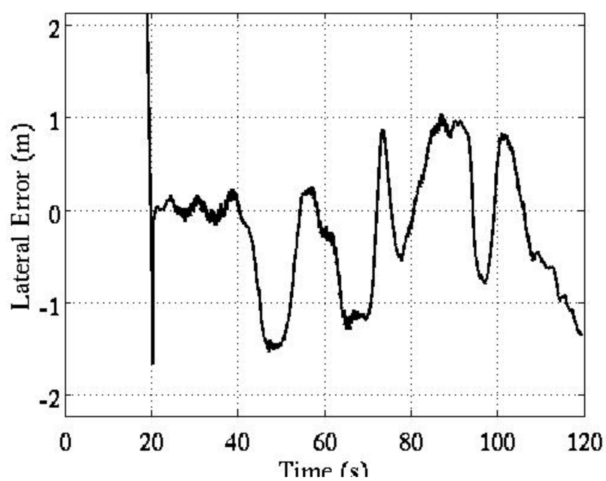

Fig. 11. The lateral error between the traveled paths of the follower and lead vehicles reaches a maximum of 1.6 meters with a 50 m following distance.

and the first point of the path traveled by the leader. Once the follower is on the path, a maximum error of 1.6 meters is observed.

While this level of error might be acceptable in some scenarios, such as a convoy operating in an open field, it is not desirable for high precision applications, such as convoying through a city making 90 degree turns or on public roads where the lane width could be as narrow as three meters. However, the Modified Extended Hitch Trailer Method does provide a means to follow a lead vehicle at large following distances. The previous methods shown fail when path complexity increases. Also, further analysis reveals that the inability to replicate the path with higher accuracy is due to the controller and not the reference point generation method.

C. Controller Limitations

The waypoint based heading controller has inherent limitations in its ability to follow a set of reference points. The most obvious shortcoming of the method is its tendency to filter curvature in the path (i.e. cut through a corner) if a reference point is chosen too far away from the vehicle. The vehicle drives to the chosen reference point using the shortest path possible. The feed forward gain in the controller can reduce this effect by generating a steer angle based on a desired yaw rate, but the reduction is mainly noticed in steady state turning maneuvers.

The second drawback to the controller is that reference points too close to the vehicle can promote marginally stable, or even unstable behavior. If the reference point is such that a large yaw error is given to the controller, a large input will be produced to turn the vehicle towards the reference point. This action causes the vehicle to drive more perpendicular to the path rather than along the path. Once the vehicle reaches the reference point, another is chosen. Due to the current orientation of the vehicle, a larger yaw error is calculated which generates a larger input. If speeds are low enough, the vehicle can oscillate about the desired path of travel. Instability is encountered when speeds are high enough that the vehicle breaches its physical limitations and either slides out or rolls over. A higher closed loop bandwidth generates larger control gains and therefore bigger inputs, so the effect can be worsened if this approach is used in an attempt to fix ill desired behavior. Also, higher control gains require higher measurement rates, which can increase system complexity and cost.

To minimize the limitations of a waypoint based controller, a "look ahead distance" was set based on the vehicle speed. The reference angle was generated by using the past location of the lead vehicle that was nearest to this distance. The look ahead distance was short at slow speeds where the possibility of a dynamic path is higher. High speeds required a longer distance to effectively filter out subtle changes in the reference points that could destabilize the vehicle.

The path duplication inaccuracies can be attributed to the "look ahead distance" having to be too large to ensure stability. Therefore when using the Modified Extended Hitch Trailer Method, some of the negative aspects of the Trailer Method and Extended Hitch Trailer Method are reacquired because the following vehicle cannot control to a sufficiently close past position of the lead vehicle. Future work will adapt this method for use in a more robust vehicle controller that can track lines instead of waypoints. This type of controller will offer more tuning capability and provide immunity to a constantly changing reference.

VII. Conclusion

A method was presented to enable a following vehicle to replicate the path driven by a lead vehicle while both are in motion and out of sight of one another. This method improved accuracy over simply following waypoints dropped by the leader. Limitations were due to the selected vehicle controller and not the method itself.

Also detailed were carrier based algorithms to determine relative position between two dynamic points and the change in position of a point. The DRTK algorithm provided a centimeter level accurate RPV, while the TDCP algorithm provided a millimeter level change in position.

Future work will alter the trajectory duplication method to work with a line tracking controller, as opposed to the current waypoint based heading controller. Also, the integer ambiguity ratio test will be replaced with a Bootstrapping method to improve the integrity of the chosen sets.

Acknowledgment

The authors would like to thank TARDEC for their support of this work.

References

[1] S. Crawford, M. Cannon, D. Ltourneau, P. Lepage, and F. Michaud, "Performance evaluation of sensor combinations on mobile robots for automated platoon control," *Proceedings of the 17th International Technical Meeting of the Satellite Division of the Institute of Navigation ION GNSS 2004*, pp. 706–717, 2004.

[2] T. C. Ng and J. I. Guzman, "Autonomous vehicle-following systems: A virtual trailer link model," in *IEEE International Conference on Intelligent Robots and Systems*, 2005.

[3] M. J. Woo, J. W. Choi, and H. S. Han, "Carrier phase gps/millimeter-wave radar for vehicle platooning," in *IEEE International Symposium on Industrial Electronics*, 2001.

[4] M. Cannon, C. Basnayake, S. Crawford, S. Syed, and G. Lachapelle, "Precise gps sensor subsystem for vehicle platoon control," *Proceedings of the 16th International Technical Meeting of the Satellite Division of the Institute of Navigation ION GPS/GNSS 2003*, pp. 213–224, 2003.

[5] C. C. Kellum, "Basic feasibility of gps positioning without carrier-phase measurements as a relative position sensor between two vehicles," *Proceedings of the 2005 National Technical Meeting of the Institute of Navigation*, pp. 903–910, 2005.

[6] S. J. Comstock, "Development of a low-latency, high data rate, differential gps relative positioning system for uav formation flight control," Ph.D. dissertation, Air Force Institute of Technology, 2006.

[7] S. Felter and N. Wu, "A relative navigation system for formation flight," *IEEE Transactions on Aerospace and Electronic Systems*, vol. 33, pp. 958–967, 1997.

[8] S. Khanafseh, B. Kempny, and B. Pervan, "New applications of measurement redundancy in high performance relative navigation systems for aviation," *Proceedings of the 19th International Technical Meeting of the Satellite Division of the Institute of Navigation ION GNSS 2006*, pp. 3024–3034, 2006.

[9] S. Dogra, J. Wright, and J. Hansen, "Sea-based jpals relative navigation algorithm development," *Proceedings of the 18th International Technical Meeting of the Satellite Division of the Institute of Navigation ION GNSS 2005*, pp. 2871–2881, 2005.

[10] T. Ford, M. Hardesty, and M. Bobye, "Helicopter ship board landing system," in *ION GNSS 18th International Technical Meeting of the Satellite Division*, 2005.

[11] M. Petovello, G. Lachapelle, and M. Cannon, "Using gps and gps/ins systems to assess relative antenna motion onboard an aircraft carrier for shipboard relative gps," *Proceedings of the 2005 National Technical Meeting of the Institute of Navigation*, pp. 219–229, 2005.

[12] T. D. Gillespie, *Fundamentals of Vehicle Dynamics*. Society of Automotive Engineers, 1992.

[13] R. Daily, W. Travis, and D. M. Bevly, "Cascaded observers to improve lateral vehicle state and tire parameter estimates," *International Journal of Vehicle Autonomous Systems*, vol. 5, pp. 230–255, 2007.

[14] P. Misra and P. Enge, *Global Positioning System: Signals, Measurements, and Performance*. Ganga-Jamuna Press, 2006.

[15] B. Hofmann-Wellenhof, H. Lichtetnegger, and J. Collins, *GPS: Theory and Practice*. Springer-Verlag, 2001.

[16] A. Gelb, *Applied Optimal Estimation*, A. Gelb, Ed. The MIT Press, 1974.

[17] C. van Loan, "Computing integrals involving the matrix exponential," *IEEE Transactions on Automatic Control*, vol. AC-14, pp. 396–404, 1978.

[18] D. Lawrence, R. B. Langley, D. Kim, F.-C. Chan, and B. Pervan, "Decorrelation of troposphere across short baselines," *Proceedings of IEEE/ION Postion, Location, and Navigation Symposium*, pp. 94–102, 2006.

[19] P. de Jonge and C. Tiberius, "The lambda method for integer ambiguity estimation: Implementation aspects," Delft Geodetic Computing Centre, Tech. Rep., August 1996.

[20] P. Joosten and C. Tiberius, "Lambda: Faqs," *GPS Solutions*, vol. 6, pp. 109–114, 2002.

[21] P. Joosten, "The lambda-method: Matlab implementation," Mathematical Geodesy and Positioning, Delft Universtiy of Technology, Tech. Rep., 2001.

[22] P. E. Henderson, "Development and testing od a multiple filter approach for precise dgps positioning and carrier phase ambiguity resolution," Master's thesis, Air Force Institute of Technology, 2001.

[23] P. Teunissen, "Success probability of integer gps ambiguity rounding and bootstrapping," *Journal of Geodesy*, vol. 72, pp. 606–612, 1998.

[24] J. Wendel, O. Meister, R. Monikes, and G. Trommer, "Time-differenced carrier phase measurements for tightly coupled gps/ins integration," in *Proceedings of IEEE/ION Postion, Location, and Navigation Symposium*, 2006, pp. 54–60.

[25] R. G. Brown and P. Y. Hwang, *Introduction to Random Signals and Applied Kalman Filtering with Matlab Exercises and Solutions*. John Wiley & Sons, Inc., 1997.

[26] B. K. Soon, S. Scheding, H.-K. Lee, H.-K. Lee, and H. Durrant-Whyte, "An approach to aid ins using time-differenced gps carrier phase (tdcp) measurements," *GPS Solutions*, 2008.

[27] E. D. Kaplan and C. J. Hegarty, *Understanding GPS: Principles and Applications*, E. D. Kaplan and C. J. Hegarty, Eds. Artech House, Inc., 2006.